Electronic and vibrational structure of transition metal trimers: Photoelectron spectra of Ni_3^-, Pd_3^-, and Pt_3^-

Kent M. Ervin, Joe Ho, and W. C. Lineberger
Department of Chemistry and Biochemistry, University of Colorado, and Joint Institute for Laboratory Astrophysics, University of Colorado and National Bureau of Standards, Boulder, Colorado 80309

(Received 27 May 1988; accepted 6 July 1988)

The transition metal trimer anions Ni_3^-, Pd_3^-, and Pt_3^- are prepared in a flowing afterglow ion source with a cold cathode dc discharge. The low-lying electronic states of the neutral trimers are probed by 488 nm negative ion photoelectron spectroscopy at an electron kinetic energy resolution of 5–12 meV. Each trimer exhibits multiple low-lying electronic states. Vibrational progressions are observed in tripalladium and triplatinum. The adiabatic electron affinities are found to be $EA(Ni_3) = 1.41 \pm 0.05$ eV, $EA(Pd_3) \lesssim 1.5 \pm 0.1$ eV, and $EA(Pt_3) = 1.87 \pm 0.02$ eV.

I. INTRODUCTION

Bare metal clusters serve as models for catalytic systems and in the quest to understand the transition between atomic or molecular properties and bulk behavior.[1-3] The properties, structure, and reactivity of metal clusters have been intensely studied for several years. Properties such as ionization potentials, electron affinities, and reactivity can now be measured for a variety of cluster species as a function of cluster size. Transition metal clusters are of special interest because of the availability of *d* orbitals for bonding. Experimental and theoretical investigation of the detailed electronic and vibrational structure of transition metal clusters has been limited primarily to dimers and a few trimers.

In this work, we present photoelectron spectra of the Group VIII A (Group 10) trimer anions Ni_3^-, Pd_3^-, and Pt_3^-. The electronic and vibrational spectra of the neutral trimers are examined within about 1 eV of their ground states. As discussed in Morse's review,[1] the bonding of transition metal trimers is expected to be dominated by molecular orbitals arising from atomic $(n+1)s$ orbitals, while the *nd* orbitals are mainly localized on the atoms. In this scheme, bonding will be controlled by the relative sizes of $(n+1)s$ and *nd* orbitals, the promotion energy required to produce the $d^m s^1$ atomic configuration, and the *d* electron exchange energy. For species on the right-hand side of the transition metal series ($m > 5$), a large number of low-lying electronic states are expected to arise from various configurations and couplings of the *nd* electron holes. The nickel, palladium, and platinum series is of particular interest because the $(n+1)s$ and *nd* orbitals of the atomic species have very similar energies, while the sizes of the *s* orbitals relative to the *d* orbitals decrease from the first to the third row.

Investigations of metal clusters using photoelectron spectroscopy have been initiated recently in our laboratory[4] and elsewhere.[5-7] Several aspects of negative ion photoelectron spectroscopy[8] make it well suited for the study of transition metal clusters. First, mass spectrometry can be used to select the cluster anion of interest, eliminating ambiguities in the signal carrier which can occur in inert gas matrix studies and in neutral cluster beams. Second, the low energy region including the ground state of the neutral species and its low-lying electronic states are accessed. Visible and ultraviolet spectroscopy of neutrals provide information about transitions to high electronic states. Third, the photoelectron spectrum is continuous over the available energy range. A disadvantage of photoelectron spectroscopy compared to other spectroscopic techniques is that the resolution is instrumentally limited to $\Delta E = 3$–20 meV (25–160 cm^{-1}) for electrostatic electron energy analyzers[9] or $\Delta E = 10$–200 meV (80–1600 cm^{-1}) for instruments with time-of-flight analyzers.[5,7,10,11] Electrostatic energy analysis, used in the present work, provides nearly constant ΔE over the accessible energy range. For time-of-flight analyzers $\Delta E/E$ is constant, so the resolution is lower at higher electron kinetic energies. The vibrational frequencies of small transition metal clusters are typically in the range 100–400 cm^{-1}. This work presents spectra of the metal trimers with the highest resolution currently attainable on a routine basis in negative ion photoelectron spectroscopy, 5–12 meV (40–100 cm^{-1}), which permits resolution of vibrational structure in favorable cases.

II. EXPERIMENTAL METHODS

The negative ion photoelectron spectrometer and metal cluster anion source have been described in detail previously.[4,12] Metal cluster anions are prepared in a flowing afterglow ion source by cathodic sputtering with a dc discharge.[4] The cathode is constructed of nickel, palladium, or platinum to produce the corresponding metal cluster anions. A flow of ~5% argon in helium is passed over the cathode with a flow tube pressure of ~0.3 Torr. The discharge is typically operated with the cathode at -3 kV with respect to the grounded flow tube and a discharge current of 10–20 mA. Cluster ions are produced from sputtering of the cathode by argon ions, possibly followed by further clustering in the discharge plasma. Collisions with the flow gas downstream from the cathode cool the ions to near room temperature. Copper and silver dimer anions produced under similar conditions have vibrational temperatures of 350 ± 50 K, as determined from hot band intensities in their photoelectron spectra.[13]

The ions are extracted from the flow tube, focused into a beam, and mass selected with a Wien filter. Ion currents of 10–30 pA of Ni_3^-, Pd_3^-, and Pt_3^- are obtained at the interac-

 0021-9606/88/204514-08$02.10

TABLE I. Adiabatic electron affinities (eV).

	Atom[a]	Trimer[b]
Nickel	1.156 ± 0.010	1.41 ± 0.05
Palladium	0.557 ± 0.008	$\lesssim 1.5 \pm 0.1$
Platinum	2.128 ± 0.002	1.87 ± 0.02
Oxygen	$1.461\,125 \pm 0.000\,010$	

[a] H. Hotop and W. C. Lineberger, J. Phys. Chem. Ref. Data **14**, 731 (1985).
[b] This work.

tion region. The mass resolution of the Wien filter is sufficient to separate Ni_3^- and Pd_3^-, from their oxides, but Pt_3^- cannot be completely separated from its oxides. However, photoelectron spectra of Pt_3^- taken on the heavy and light sides of the triplatinum mass peak are identical. This indicates that oxides of Pt_3^- either are not produced by the source or do not photodetach at the photon energy used.

The mass-selected ions are crossed by the intracavity 488 nm radiation of a cw argon ion laser, with a circulating power of 80 W at the interaction region. The kinetic energy of the photodetached electrons is measured with a hemispherical electrostatic energy analyzer operated at a transmission energy of 1.5 eV. The instrumental resolution is 5–7 meV (40–60 cm^{-1}) FWHM for the nickel and palladium spectra and 8–12 meV (70–100 cm^{-1}) for the platinum spectrum. The polarization of the laser light is fixed at the "magic angle" relative to the direction of the electron detector, such that the signal intensities are proportional to the average photodetachment cross sections.[12] The electron kinetic energy scale is calibrated with respect to the known electron affinities of atomic oxygen and atomic Ni, Pd, or Pt (Table I) from transitions in the photoelectron spectra of the corresponding anions. The uncertainty of the absolute electron kinetic energies is ± 5 meV.

III. RESULTS AND ANALYSIS

Figure 1 presents the 488 nm photoelectron spectra of Ni_3^-, Pd_3^-, and Pt_3^-. Distinguishable features in each spectrum are labeled in Fig. 1 and peak positions are listed in Table II. The experimental uncertainties of the peak positions are ± 30 cm^{-1} for sharp peaks and ± 60 cm^{-1} for weak peaks and shoulders. The widths of the sharper vibrational peaks in Pd_3 (C–G,J,K) and Pt_3 (B,D,G,H) are in the range of 15–30 meV, significantly broader than the instrumental linewidth. Rotational broadening for these heavy species is expected to contribute less than 1 meV to the observed widths. The observed broadening is primarily due to overlapping electronic states and vibrational progressions, and to unresolved sequence bands.

Each spectrum exhibits several features which correspond to low-lying electronic states of the neutral trimers. Trinickel has only diffuse features with no vibrational structure apparent on the scale of Fig. 1. Both broad features and sharp vibrational progressions are observed in tripalladium. Triplatinum exhibits just two main bands, each with several sharp peaks.

The low vibrational frequencies for heavy metal clusters (100–400 cm^{-1}), the instrumental linewidth of 40–100 cm^{-1}, the presence of electronically and vibrationally excited anions, and overlapping low-lying electronic states all contribute to a limited ability to distinguish individual tran-

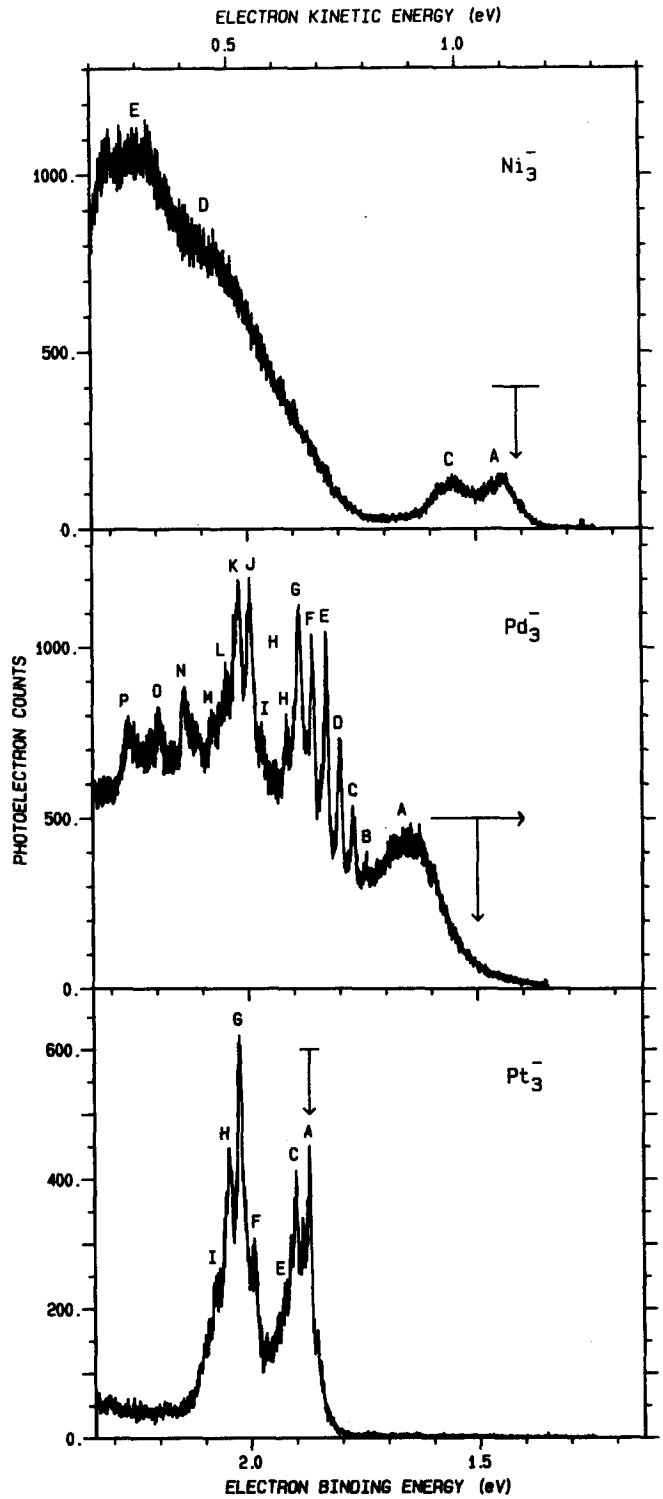

FIG. 1. Photoelectron spectra of the metal trimer anions Ni_3^- (top), Pd_3^- (middle), and Pt_3^- (bottom). The photoelectron counts are plotted vs the electron binding energy (lower scale), given by the photon energy (2.54 eV at 488 nm) minus the measured electron kinetic energy (upper scale). The vertical arrows indicate the assigned adiabatic electron affinities, given in Table I, with horizontal lines indicating the uncertainty limits. Peak labels refer to Table II.

TABLE II. Summary of spectral features.

Trimer	Peak[a]	eKE (eV)[b]	Spacing (cm^{-1})[c]
Ni_3	A	1.100	
			210
	B	1.074	
	C	0.97	
	D	0.45	
	E	0.30	
Pd_3	A	0.885	
			223
	B	0.796	
			230
	C	0.768	
			241
	D	0.739	
			236
	E	0.710	
			236
	F	0.680	
			(219)
	G	0.651	
	H	(0.624)	
			(185)
	I	(0.567)	
			211
	J	0.544	
			(209)
	K	0.518	
			(220)
	L	(0.492)	
	M	(0.465)	
	N	0.401	
	O	0.346	
	P	0.281	
Pt_3	b	(0.697)	
			(113)
	a	(0.683)	
			(97)
	A	0.671	
			97
	B	0.659	
			137
	C	0.642	
			(113)
	D	(0.628)	
			(104)
	E	(0.615)	
	F	0.550	
			250
	G	0.519	
			177
	H	0.497	
			(186)
	I	(0.474)	

[a]Peak labels refer to Figs. 1–3.
[b]Peak position, electron kinetic energy. Experimental uncertainty is $\pm$ 0.005 eV ($\pm$ 0.010 for values in parentheses).
[c]Experimental uncertainty $\pm$ 30 cm^{-1} ($\pm$ 60 cm^{-1} for values in parentheses).

sitions. In addition, spin–orbit couplings and Jahn–Teller couplings may give rise to unresolved splittings. A consequence of this spectral congestion is that definite assignment of the various features is difficult at best, and unresolved or weak transitions may escape identification. The three trimers are considered individually below.

A. Trinickel

The spectrum of trinickel, Fig. 1, shows two features (A and C) at low binding energies with a separation of 0.13 eV and approximate widths of 0.1 eV, and a broad photodetachment band beginning 0.4 eV above A and extending to the limit of the photon energy. The broad feature shows some structure, but is likely composed of many overlapping electronic states. Peaks A and C are a factor of 7 less intense than the broad feature, but it is unlikely that they are due to excited states of the anion, since in that case their intensities would be expected to be much smaller. No change was observed in the relative intensities of the A and C features when ion source conditions were varied (however, this diagnostic is not definitive because the vibrational temperatures of transition metal dimer anions produced by the source are also largely invariant with respect to source conditions[4,13]).

A closeup of the Ni_3 spectrum in the region of ground state is presented in Fig. 2. Figure 2 shows that the feature at lowest binding energy actually consists of two peaks (A and B) separated by 210 $\pm$ 30 cm^{-1}. Although the two peaks are only partially resolved and the signal-to-noise level of the spectrum is low, these features proved to be reproducible. The sharp peaks in Fig. 2 are attributed to a two-photon process, as discussed below. A possible assignment of the A and B peaks, separated by 210 $\pm$ 30 cm^{-1}, is to a vibrational progression of the ground state of Ni_3. Moskovits and DiLella[14] observed the resonance Raman spectrum of Ni_3 in argon matrices, and found a symmetric stretch frequency of $\nu_1 = 232.3\ cm^{-1}$. Isotopic analysis indicated that Ni_3 in argon has C_{2v} symmetry with an bond angle of 90° to 100°. Gole[15] recently reported the visible spectrum of Ni_3 in the gas phase, and found ground state frequencies of $\nu_1 = 230 \pm 5\ cm^{-1}$ and (tentatively) $\nu_2 = 100 \pm 5\ cm^{-1}$ for the bending mode. Nour *et al.*[16] reported the far infrared spectrum of nickel clusters in an argon matrix and identified a transition at 198 cm^{-1} as the ν_3 antisymmetric stretch mode of Ni_3. Both the symmetric stretch and bend modes are expected to be active in the photoelectron spectrum for a C_{2v} molecule. The observed A–B separation agrees with the symmetric stretch frequency of Ni_3 within experimental uncertainty. An unresolved vibrational progression at a lower frequency, unresolved sequence bands, and partial overlap

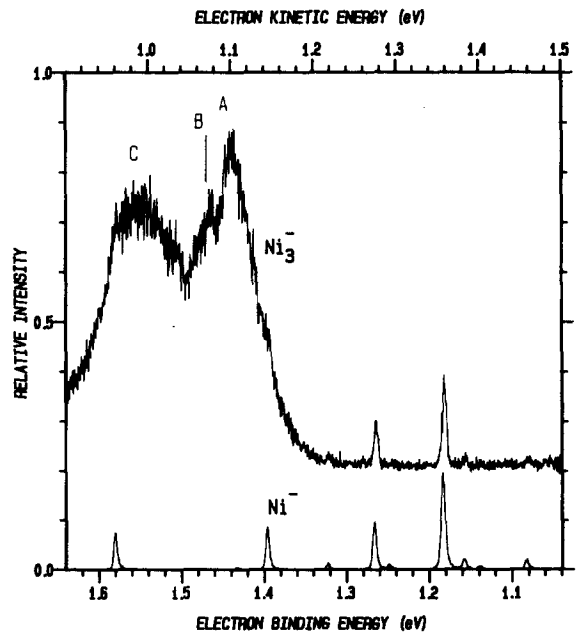

FIG. 2. Photoelectron spectrum of atomic Ni^- (lower trace) and Ni_3^- (upper trace, offset from zero). The photoelectron counts are plotted vs the electron binding energy (lower scale), given by the photon energy (2.54 eV at 488 nm) minus the measured electron kinetic energy (upper scale). The narrow peaks in the trinickel spectrum are attributed to photodetachment of Ni^- formed from photodissociation of Ni_3^- in a two-photon process. The vertical scales for Ni^- and Ni_3^- are normalized to give equal heights for the atomic transitions. Peak labels refer to Table II.

with peak C could account for the lack of sharp features. However, attempts to model the Franck–Condon profile of the A and B features (using reasonable estimates for the molecular constants) indicate that sharper features probably would be observable at the instrumental resolution if a single electronic transition were responsible for the photodetachment.

A more probable explanation for the observed spectrum is that several low-lying, nearly degenerate electronic states overlap to account for the A and B features. Walch[17] has carried out *ab initio* calculations for six low-lying electronic states of trinickel. Five states, four with near-equilateral and one with linear geometry, were estimated to be within 0.05 eV (400 cm^{-1}). The ground state could not be definitively identified at the level of the calculations. Previous calculations[18–20] varied in the assignment of the ground state as linear or triangular. Walch's low-lying states have calculated symmetric stretch frequencies of 180–260 cm^{-1} and bend frequencies of 80–150 cm^{-1}. Overlapping vibrational progressions from these electronic states—and additional contributions from populated electronic states of the anion in the same energy range—can easily account for the observed diffuse nature of these bands. Walch[17] also calculated a sixth state with an estimated excitation energy of 0.13–0.17 eV above the five nearly degenerate states. This corresponds nicely with the observed position of the *C* band. Thus, the observed spectrum is consistent with Walch's calculations, although the lack of resolved transitions precludes a definitive test.

The determination of the electron affinity of trinickel depends on our estimate of the position of the unresolved ground state vibrational origin. Rough Franck–Condon simulations of the A–B band indicate reasonable positions of the vibrational origin are in the range 1.40–1.44 eV. The onset of the photodetachment signal at 1.33 eV, plus a thermal correction of 0.03 eV, provides a lower limit 1.36 eV. We estimate that the adiabatic electron affinity is in the range $EA(Ni_3) = 1.41 \pm 0.05$ eV.

Figure 2 also shows a series of isolated, sharp peaks at electron binding energies below that of feature A. These correspond to photodetachment of atomic Ni^- in a two-photon process in which photodissociation, $Ni_3^- + h\nu \rightarrow Ni^- + Ni_2$, is followed by photodetachment, $Ni^- + h\nu \rightarrow Ni + e^-$. The peak positions correspond exactly to those seen in the photoelectron spectrum of free Ni^-, which is shown in Fig. 2 for comparison. The linewidths of the atomic transitions are limited by the instrumental resolution. Within experimental uncertainty, the relative intensities of the Ni^- transitions observed in the Ni_3^- spectrum are the same as for free Ni^-. An attempt to measure the laser power dependence of the atomic peak intensities to verify a two-photon process was inconclusive because of low signal levels. It is unlikely, however, that Ni^- is formed by decomposition of metastable Ni_3^- because (1) the predissociative anions should be quenched during the many collisions in the flowing afterglow ion source and because (2) a predissociation lifetime of 10^8 vibrational periods would be required for such a process to be observed. The two-photon process occurs during the ~20 ns transit time of the ion through the laser field. We do not detect photodetachment from Ni_2^- (which has a transition at an electron binding energy of 0.93 eV)[13] in the photoelectron spectrum of Ni_3^-.

Observation of photodissociation of Ni_3^- places a strict upper limit on the dissociation energy, $D_0(Ni_2\text{–}Ni^-) < h\nu = 2.54$ eV. Using the relation $EA_3(Ni_3) + D_0(Ni_2\text{–}Ni) = EA(Ni) + D_0(Ni_2\text{–}Ni^-)$ and the trimer electron affinity measured here (Table I), this gives $D_0(Ni_2\text{–}Ni) < 2.26 \pm 0.05$ eV. This limit compares with theoretical estimates[18,20] of $D_0(Ni_2\text{–}Ni)$ of 1.3–2.3 eV. Thermochemical considerations indicate that Ni_2 is the neutral product in the initial photodissociation. Given $D_0(Ni_2) = 2.07$ eV,[1] photodissociation of Ni_3^- into three atoms would imply $D_0(Ni_2\text{–}Ni^-) < 0.47$ eV and $D_0(Ni_2\text{–}Ni) < 0.21$ eV, which is an unreasonably small value.

B. Tripalladium

The photoelectron spectrum of tripalladium exhibits a rich spectrum comprising resolved vibrational progressions along with diffuse electronic bands. To our knowledge, no other experimental observations or theoretical calculations have been reported for tripalladium.

The feature with lowest electron binding energy, peak A (Fig. 1 and Table II), shows no resolved vibrational structure. It is approximately 0.2 eV wide, twice that of the lowest bands in trinickel. Assuming feature A corresponds to a single electronic state (which the present experiments cannot substantiate), the width would indicate that the transition involves a large change in molecular geometry between the anionic and neutral species. Peak A exhibits a long tail towards low electron binding energy, which suggests that the vibrational origin may be weak because of a small Franck–Condon overlap. Since no molecular constants are known, no Franck–Condon simulation of the band was attempted. An upper limit for the adiabatic electron affinity is given by the onset of photodetachment, $EA(Pd_3) \lesssim 1.5 \pm 0.1$ eV.

An extended vibrational progression is observed at electron binding energies between 1.7 and 1.9 eV. Peaks B through H are almost evenly spaced, separated by an average 230 cm^{-1}. Peak G is anomalously intense and has a greater width compared to peaks B through F, probably indicating that an additional electronic transition arises near peak G. Because of the overlapping broad photodetachment, it is impossible to identify a vibrational origin for the B through F progression. The extended progression qualitatively indicates a large geometry change for this electronic transition. Another more or less regular progression is observed at electron binding energies between 1.98 and 2.07 eV, peaks I through M (see Table II). It is uncertain whether a single electronic state is responsible for these transitions.

C. Triplatinum

The photoelectron spectrum of triplatinum, Fig. 1, shows two main bands peaking at electron binding energies of 1.87 and 2.02 eV, each with several sharp features. Figure 3 shows an expanded view of this region of the spectrum.

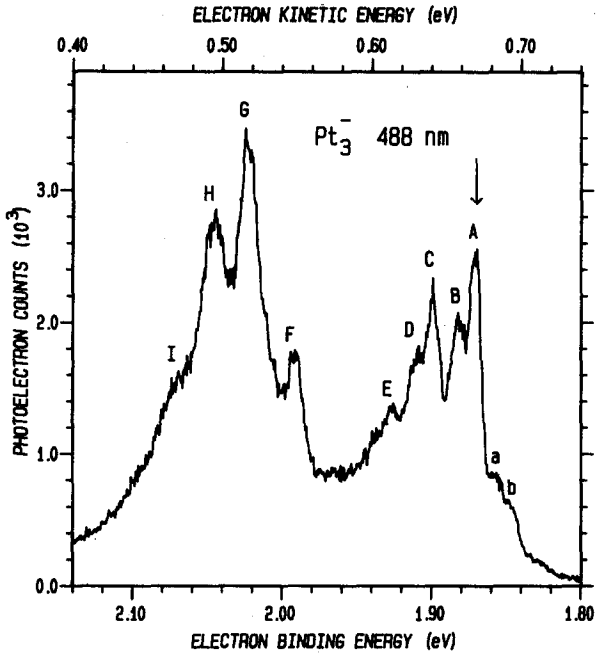

FIG. 3. Photoelectron spectrum of Pt_3^-. The photoelectron counts are plotted vs the electron binding energy (lower scale), given by the photon energy (2.54 eV at 488 nm) minus the measured electron kinetic energy (upper scale). Peak labels refer to Table II. The arrow indicates the assigned vibrational origin.

We identify peak A (Fig. 3 and Table II) as the vibrational origin of the ground state. The shoulders (a and b) to the right of peak A are characteristic of vibrational hot bands in that they are much weaker than peak A; a Franck–Condon progression beginning with a or b and including peak A would have to be much more extended than the observed progression. The shoulders a and b have intensities consistent with populations at the expected vibrational temperature of 350 ± 50 K. We cannot, however, rule out the possibility that a or b could be due to separate electronic transitions.

Two characteristic peak spacings are found in the lowest band of triplatinum: A–B and C–D have spacings of $105 \pm 30\,cm^{-1}$ and A–C and C–E have spacings of 225 ± 30 cm^{-1}. There are two satisfactory assignments: (1) One possibility is that the whole progression consists of a single electronic state with two active modes, A→C and C→E corresponding to a symmetric stretch and A→B and C→D to bending modes. (2) Alternatively, peak C could correspond to a low-lying electronic state. In this case, each of the two states has a vibrational mode with frequency 105 ± 30 cm^{-1}. One might expect a lower frequency for Pt_3 relative to Ni_3 because of the higher mass, which would favor the second alternative, but on the other hand the expected increased role of *d* orbitals in bonding for the third row relative to the first row might increase the bond strength and therefore the vibrational frequency. An *ab initio* calculation of sufficient quality to distinguish between a $\sim 105\,cm^{-1}$ and a $\sim 225\,cm^{-1}$ vibrational frequency would aid in the assignment of the spectrum. The only available calculations[21,22] for bare platinum clusters fixed the Pt–Pt interatomic distances at the bulk value and did not predict frequencies. For either choice of assignments, the vibrational progression peaks in intensity at the vibrational origin, indicating that the Franck–Condon geometry change between the anion and neutral species is not large. Based upon our assignment of peak A as the ground state origin, the adiabatic electron affinity of triplatinum is $EA(Pt_3) = 1.87 \pm 0.02$ eV.

The second main group of transitions in the spectrum consists of peaks F through I. We tentatively assign these to a vibrational progression of a single electron state. In that case, peak G corresponds to the vibrational origin, G→H→I is a vibrational progression with frequency $\sim 180\,cm^{-1}$, and peak F corresponds to a vibrational hot band with frequency $\sim 250\,cm^{-1}$. However, we cannot exclude the possibility that the peaks correspond to two or more low-lying and closely spaced electron states.

The photodetachment signal is nonzero at electron binding energies above the two main features. This behavior is reminiscent of the onset of the higher energy diffuse bands in the trinickel spectrum, suggesting similar bands in triplatinum at energies beyond the range of the present experiments.

IV. DISCUSSION

A simple generalization that can be drawn from the observed photoelectron spectra is that each of the nickel group transition metal trimers has a number of low-lying electronic states. A high density of states has been predicted for transition metal molecules with open *d* shells.[1,23,24] The observation of multiple low-lying states is of some importance since there has been a conflict between the predicted density of states and the number of states seen in photoelectron spectra of transition metal dimers. In Fe_2, *ab initio* electronic structure calculations[25] predicted 112 electron states within 0.5 eV of the ground state, but only two low-lying electronic states were observed in the photoelectron spectrum.[26] More recent *ab initio* calculations[27] on Fe_2 indicate that larger basis sets and more extensive configuration interaction lead to greater *d–d* interaction and a reduction in the number of electronic states. However, more than two low-lying states are still predicted. Leopold *et al.*[28] have reinterpreted the Fe_2 spectrum in terms of neutral states arising from mixed atomic asymptotes ($3d^6\,4s^2 + 3d^7\,4s^1$), a configuration not yet considered in *ab initio* calculations.

Walch and Bauschlicher[23] have performed *ab initio* calculations on Cu_3 and transition metal trimers on the left-hand side of the periodic table, and Walch[17] has recently presented calculations for low-lying states of trinickel. The qualitative molecular orbital picture of the bonding which emerges from these calculations will be applied to the present results. The *ab initio* calculations generally agree that the atomic $(n+1)s$ orbitals dominate the bonding, while the *nd* electrons remain fairly localized on the atoms and are largely nonbonding. This qualitative bonding scheme is most likely for the first row, where the 4*s* orbitals are large compared to the 3*d* orbitals, but less so for the second and third rows, where the $(n+1)s$ and *nd* orbitals are of more comparable radial extent. The occupation of *s*- or *d*-derived molecular

TABLE III. Atomic energy levels (eV)[a].

	Ni	Pd	Pt
d^{10}	1.82	0.00	0.76
d^9s^1	0.09	0.95	0.04
d^8s^2	0.12	3.38	0.10

[a]Averaged over J levels. C. E. Moore, *Atomic Energy Levels*, Natl. Stand. Ref. Data Ser. Circ. 467 (U.S. GPO, Washington, D.C., 1948).

orbitals is determined by the balance among promotion energy to the $d^m s^1$ atomic configuration, bonding of the s-derived molecular orbitals, and the d-electron exchange energy.

Walch's calculations[17] indicate that equilateral triangular and linear geometries are nearly degenerate for trinickel. The molecular orbital occupancies are given by $(d_A)^9(d_B)^8(d_C)^9(sp\sigma_g)^2(sp\sigma_u)^2$ (linear) and $(d_A)^9(d_B)^9(d_C)^9(sa_1')^2(se')^1$ (equilateral triangle). We represent the d electrons the atomic limit, where A, B, and C simply label the individual atoms and B is the central atom in the linear case. Jahn–Teller coupling distorts the triangular species away from equilateral geometry.[17] In the linear configuration, the d^8s^2 configuration is favored for the central atom, since this allows s–p hybridization and formation of two full bonds with the outer atoms. This extra bonding compensates for the required $s \rightarrow p$ promotion energy.[17] Energies for selected atomic electron configurations are given in Table III. For nickel atom the d^9s^1 and d^8s^2 configurations are essentially degenerate, which partly explains why the linear and triangular geometries have nearly the same energy. For palladium, on the other hand, d^{10} is the ground state, a 0.95 eV promotion energy is required to form d^9s^1, and a significantly higher promotion energy is required for d^8s^2 (see Table III). The high promotion energy for d^8s^2 favors the triangular geometry in Pd_3. In platinum, the d^9s^1 and d^8s^2 configurations are again nearly degenerate, so the linear and triangular forms of triplatinum may have similar energies. Calculations indicate that relativistic effects have a profound influence on energy levels and bonding in platinum dimer[29] and higher platinum clusters.[21]

The bonding scheme in the anion trimers is expected to be very similar to that of the neutrals. The atomic anions[10] have d^9s^2 ground states for Ni^- and Pt^- and near-degenerate d^9s^2 and $d^{10}s^1$ lowest states for Pd^-. The combination of an d^9s^2 anion with two d^9s^1 neutral atoms leads to the molecular orbital occupancies $(d_A)^9(d_B)^9(d_C)^9(sp\sigma_g)^2(sp\sigma_u)^2$ (linear) and $(d_A)^9(d_B)^9(d_C)^9(sa_1')^2(se')^2$ (equilateral). The linear configuration is favored for the anionic trimers because no promotion energy is required to reach the $d^m s^2$ configuration for the central M^- atom, and because four electrons in the sp molecular orbitals of the linear molecule provide more bonding than in the triangular molecule, for which the se' orbitals are mainly nonbonding.[30] Detachment from an $sp\sigma$ orbital in the linear configuration, however, does not lead to the ground state configuration of the linear neutral in a one electron process. Detachment of an se' electron from the equilateral geometry, on the other hand, would lead to the ground equilateral configuration of the neutral via a vertical transition. The observation of fairly narrow Franck–Condon profiles for the lowest states in Ni_3 and Pt_3, but wider bands and progressions for Pd_3 suggests nonvertical transitions in the latter case, i.e., linear $Pd_3^- \rightarrow$ triangular Pd_3. The present experiments are not definitive on this point, however, and further experiments and theoretical calculations will be required to determine the anion trimer structures. As with the neutrals, a number of low-lying electronic states of the anions may arise from different configurations of the d electrons. Anion excited states within 0.1 eV are likely to be populated under the conditions of the present experiments and may contribute to the congested nature of the photoelectron spectra.

The d electrons influence bonding in the trimers as a result of d–d overlap (small for nickel, larger for palladium and platinum), exchange energy, and mixing between the s-derived bonding orbitals and d-derived molecular orbitals of the same symmetry.[23] In the limiting case that the major contribution to bonding comes from s-derived molecular orbitals, various configurations and couplings of the atomic d electrons give rise to a plethora of low-lying electronic states. Greater interactions of the d orbitals will lead to larger spacings of the electronic energy levels and a decrease in the number of low-lying electronic states. As discussed above, Walch[17] found six states within 0.2 eV for trinickel. No high-level calculations of tripalladium and triplatinum electronic states are available. In the case of dimers, all electron Hartree–Fock configuration interaction calculations[24] predict 30 electronic states within 0.6 eV of the ground state for both Ni_2 and Pd_2. For platinum dimer,[29] relativistic effects tend to spread out the energy levels of lowing-lying electronic states, but there are still a number of states predicted within 0.5 eV. The broad, diffuse features in the spectra for trinickel are consistent with a large number of overlapping electronic states. As a qualitative trend, the spectra become progressively less congested for tripalladium, which has both broad features and resolved vibrational progressions, and triplatinum, which exhibits a small number of progressions. This trend probably reflects the increased role of d electrons in the bonding as the relative sizes of the d orbitals increase from the first to the third row transition metals.

An alternative to attempting to sort out the individual electronic or vibrational transitions in the photoelectron spectra is to consider the intensities as a reflection of the overall density of states. This approach has been useful in the interpretation of bulk photoelectron spectra,[31] where the density of states is related to the electronic band structure. While it is certainly valid to state that the congested photoelectron spectra we observe are due to a large number of low-lying electronic states, it is not valid to identify photodetachment intensities directly with the density of states as a function of energy. Several factors make the photodetachment intensities differ from the density of states. The first is the Franck–Condon overlap between the anion and neutral. Franck–Condon factors will vary the most for small clusters with different geometries for the anion and neutral. Very large clusters will have less dramatic geometric variation

with charge state. Second, the photodetachment probability will vary with the orbital of the detached electrons.[32] Qualitatively, this is a consequence of the size and angular distribution of the orbital from which the electron is detached. For transition metal atoms, e.g., detachments of d electrons from the anions are typically a factor of 5–20 weaker than s electron detachments.[33] For transition metal hydrides (MH^-, M = Cr, Mn, Fe, Co, Ni), in contrast, detachment intensities of $4s\sigma$ and $3d$-type electrons have comparable intensities.[34] Finally, some states of the neutral cluster may not be accessible via a one-electron detachment process from the anion. Transitions involving a two-electron rearrangement are much weaker than one-electron processes (except where correlation effects[35] dominate).

For these reasons, caution should be exercised when interpreting the photoelectron spectra in terms of densities of states. In particular, the band intensities cannot be directly related to the number of electrons in the anion orbital from which the detachment originates. Rather, theoretical models must consider the photodetachment probabilities as well as the density of states, at least in an approximate manner. Comparable deviations between the density of states and the photoelectron intensities exist for bulk metals.[31] The availability of unfilled (conduction band) states and the transition probability between filled and unfilled states both influence the photoelectron intensities. Rather extensive calculations are required to relate the observed photoelectron spectra to the true density of states.[31] An additional effect in the photoelectron spectroscopy of bulk metals is the scattering of the electron as it escapes the metal lattice. An analogous phenomenon may exist for very large metal clusters, but is not of importance for trimers.

V. CONCLUSIONS

The photoelectron spectra of Ni_3^-, Pd_3^-, and Pt_3^- have been observed. The adiabatic electron affinities of trinickel, tripalladium, and trinickel are 1.41 ± 0.05 eV, $\lesssim 1.5 \pm 0.1$ eV, and 1.87 ± 0.02 eV, respectively. The photoelectron spectrum of each trimer exhibits transitions corresponding to multiple low-lying electronic states of the neutral trimers. The spectrum of trinickel is consistent with the *ab initio* calculations of Walch,[17] which predict six low-lying states within 0.2 eV of the ground state. A large number of low-lying electronic states is predicted for transition metal clusters with open d shells when the d orbitals are localized on the atoms. The apparent density of electronic states decreases from trinickel to tripalladium to triplatinum. This reflects an increase in the degree of bonding from the d orbitals due to the increase in the relative overlap of the d orbitals from the first to third row.

The present investigations indicate that negative ion photoelectron spectroscopy can, in favorable cases, resolve vibrational structure in transition metal clusters larger than dimers. Vibrational progressions for tripalladium and triplatinum show characteristic frequencies in the range 100–250 cm^{-1}. Low frequency vibrational modes and low-lying electronic states lead to spectral congestion, however, which limits our ability to assign individual states and transitions. The observed spectra identify regions of interest for high resolution spectroscopic investigations of these species and provide a challenge for theoretical treatments.

Further studies of transition metal clusters are in progress. Improvements in the photoelectron spectrometer have recently been implemented[36] which permit operation in the near ultraviolet (351–364 nm), a 1 eV extension of the accessible energy range. In addition, routine measurements of the angular distribution of the photodetached electrons are now possible. Since electrons detached from molecular orbitals of different symmetries are expected to have different angular distributions,[37] the latter improvement should provide an additional means to distinguish transitions belonging to different electronic states.

ACKNOWLEDGMENT

This research is supported by National Science Foundation Grant Nos. CHE 83-16628 and PHY 86-04508.

[1] M. Morse, Chem. Rev. **86**, 1049 (1986).
[2] *Metal Clusters*, edited by M. Moskovits (Wiley, New York, 1986).
[3] M. Kappes, Chem. Rev. **88**, 369 (1988).
[4] D. G. Leopold, J. Ho, and W. C. Lineberger, J. Chem. Phys. **86**, 1715 (1987).
[5] C. L. Pettiette, S. H. Yang, M. J. Craycraft, J. Conceicao, R. T. Laaksonen, O. Cheshnovsky, and R. E. Smalley, J. Chem. Phys. **88**, 5377 (1988); O. Cheshnovsky, S. H. Yang, C. L. Pettiette, M. J. Craycraft, and R. E. Smalley, Rev. Sci. Instrum. **58**, 2131 (1987); O. Cheshnovsky, S. H. Yang, C. L. Pettiette, M. J. Craycraft, Y. Liu, and R. E. Smalley, Chem. Phys. Lett. **138**, 119 (1987).
[6] K. H. Bowen (to be published).
[7] W. Begemann, S. Dreihöfer, G. Ganteför, K. H. Meiwes-Broer, and H. O. Lutz, in *Elemental and Molecular Clusters*, Springer Series on Material Science (Springer, Berlin, in press), Vol. 8; G. Ganteför, K. H. Meiwes-Broer, and H. O. Lutz, Phys. Rev. A **37**, 276 (1988).
[8] R. D. Mead, A. E. Stevens, and W. C. Lineberger, in *Gas Phase Ion Chemistry, Vol. 3 (Ions and Light)*, edited by M. T. Bowers (Academic, Orlando, 1984), pp. 213–248.
[9] H. Hotop and W. C. Lineberger, J. Phys. Chem. Ref. Data **14**, 731 (1985).
[10] L. A. Posey, M. J. Deluca, and M. A. Johnson, Chem. Phys. Lett. **131**, 170 (1986).
[11] R. B. Metz, T. Kitsopoulos, A. Weaver, and D. M. Neumark, J. Chem. Phys. **88**, 1463 (1988).
[12] D. G. Leopold, K. K. Murray, A. E. Stevens Miller, and W. C. Lineberger, J. Chem. Phys. **83**, 4849 (1985).
[13] K. M. Ervin, J. Ho, and W. C. Lineberger (unpublished).
[14] M. Moskovits and D. P. DiLella, J. Chem. Phys. **72**, 2267 (1980).
[15] J. R. Woodward, S. H. Cobb, and J. L. Gole, J. Phys. Chem. **92**, 1404 (1988).
[16] E. M. Nour, C. Alfaro-Franco, K. A. Gingerich, and J. Laane, J. Chem. Phys. **86**, 4779 (1987).
[17] S. P. Walch, J. Chem. Phys. **86**, 5082 (1987).
[18] A. B. Anderson, J. Chem. Phys. **64**, 4046 (1976); **66**, 5108 (1977).
[19] H. Basch, M. D. Newton, and J. W. Moskowitz, J. Chem. Phys. **73**, 4492 (1980).
[20] G. Pacchioni and P. Fantucci, Chem. Phys. Lett. **134**, 407 (1987).
[21] B. Bigot and C. Minot, J. Am. Chem. Soc. **106**, 6601 (1984).
[22] A. Gavezzotti, G. F. Tantardini, and H. Miessner, J. Phys. Chem. **92**, 872 (1988).
[23] S. P. Walch and C. W. Bauschlicher, in *Quantum Chemistry: The Challenge of Transition Metals and Coordination Chemistry*, edited by A. Veillard (Reidel, Dordrecht, 1986), p. 119.
[24] I. Shim, in *Understanding Molecular Properties*, edited by J. Avery (Reidel, Dordrecht, 1987), p. 555.
[25] I. Shim and K. A. Gingerich, J. Chem. Phys. **77**, 2490 (1982).
[26] D. G. Leopold and W. C. Lineberger, J. Am. Chem. Soc. **108**, 1379 (1986).
[27] M. Tomonari and H. Tatewaki, J. Chem. Phys. **88**, 1828 (1988).

[28]D. G. Leopold, J. Almlöf, W. C. Lineberger, and P. R. Taylor, J. Chem. Phys. **86**, 3780 (1988).
[29]K. Balasubramanian, J. Chem. Phys. **87**, 6573 (1987).
[30]C. W. Bauschlicher, Jr., S. R. Langhoff, and P. R. Taylor, J. Chem. Phys. **88**, 1041 (1988).
[31]A. Hamnett and A. F. Orchard, in *Electronic Structure and Magnetism of Inorganic Compounds*, edited by P. Day (Chemical Society, London, 1974), Vol. 3, p. 218.
[32]P. A. Cox and F. A. Orchard, Chem. Phys. Lett. **7**, 273 (1970); P. A. Cox, S. Evans, and A. F. Orchard, *ibid.* **13**, 386 (1972).
[33]C. S. Feigerle, R. R. Cordermann, S. V. Bobashev, and W. C. Lineberger, J. Chem. Phys. **74**, 1580 (1981).
[34]A. E. Stevens, C. S. Feigerle, and W. C. Lineberger, J. Chem. Phys. **78**, 5420 (1983); A. E. Stevens Miller, C. S. Feigerle, and W. C. Lineberger, *ibid.* **87**, 1549 (1987).
[35]L. S. Cederbaum, W. Domcke, J. Shirmer, and W. Von Niessen, Adv. Chem. Phys. **65**, 115 (1986).
[36]K. M. Ervin, J. Ho, and W. C. Lineberger, J. Phys. Chem. (in press).
[37]J. Cooper and R. M. Zare, J. Chem. Phys. **48**, 942 (1968); N. Chandra, Phys. Rev. A **36**, 3163 (1987).